Resonance fluorescence spectra of three-level atoms in a squeezed vacuum

M. R. Ferguson, Z. Ficek, and B. J. Dalton
Department of Physics, The University of Queensland, Brisbane, Queensland 4072, Australia
(Received 2 October 1995; revised manuscript received 6 March 1996)

The fluorescence field from one of the two allowed transitions in a three-level atom can sense squeezed fluctuations of a vacuum field coupled to the other transition. We examine the fluorescence spectra of strongly driven three-level atoms in Λ, V, and cascade configurations in which one of the two one-photon transitions is coupled to a finite-bandwidth squeezed vacuum field, when the bandwidth is much smaller than the difference in the atomic transition frequencies, though much larger than atomic decay rates and Rabi frequencies of the driving fields. The driving fields are on one-photon resonance, and the squeezed vacuum field is generated by a degenerate parameter oscillator. Details are only given for the Λ configuration. The extension to the V and cascade configurations is straightforward. We find that in all configurations the fluorescence spectra of the transition not coupled to the squeezed vacuum field are composed of five lines, one central and two pairs of sidebands, with intensities and widths strongly influenced by the squeezed vacuum field. However, only the central component and the outer sidebands exhibit a dependence on the squeezing phase. We also examine the fluorescence spectrum for the cascade configuration with a squeezed vacuum field on resonance with the two-photon transition between the ground and the most excited states and now generated by a nondegenerate parametric oscillator. In this case, where the squeezed vacuum field can be made coupled to both transitions, all spectral lines depend on the squeezing phase. The spectral features are explained in terms of the dressed-atom model of the system. We show that the coherent mixing of the atomic states by the strong driving fields modifies transition rates between the dressed states, which results in the selective phase dependence of the spectral features. [S1050-2947(96)05908-2]

PACS number(s): 42.50.Dv, 32.80.−t

I. INTRODUCTION

One of the more interesting developments in recent years is the possibility of an experimental observation of squeezing-induced modifications in the fluorescence light emitted by three-level atoms. In particular, an experiment has already been performed on squeezing-modified two-photon absorption in atomic cesium [1]. Recent studies of three-level atoms in the cascade configurations interacting with a squeezed vacuum field [2–5] show that the correlated pairs of photons characteristic of squeezed fields can lead to the population of the upper level having a linear dependence on intensity. This is in stark contrast to the usual quadratic dependence for a two-photon process [6]. Other interesting modifications of the radiative properties of atoms in the presence of a squeezed vacuum field have also been predicted [7]. Examples include inhibition of the atomic decay process [8], level shifts [9–12], squeezing-induced transparency [13], asymmetrics and dispersive profiles in the fluorescence spectrum [14], selective population of the atomic levels [15–17], amplification without population inversion [18], and probe absorption spectra [19].

The modifications of the dipole decay process in a two-level atom can introduce significant changes in intensities and linewidths of the fluorescence and absorption spectra. In particular, it is now well known [20–22] that the linewidths of the spectral features strongly depend on the relative phase between the squeezed vacuum and a driving field, and can be broadened or narrowed compared to that in the ordinary vacuum. Similar features have been found for multiatom resonance fluorescence [23–25] and for three-level atoms coupled to two independent squeezed vacua [26,27].

It has been pointed out, however, that these features could be difficult to observe experimentally for the following reasons. First, most of these calculations have been performed assuming that the atoms interact with a broadband squeezed vacuum. In the frequency domain, this assumption requires the bandwidth of the squeezed vacuum to be much greater than both Rabi frequencies of the driving fields and the natural linewidths of the atomic transitions. In practice, squeezing bandwidths are far from broadband. Recent studies of the effects of finite-bandwidth squeezed light on the fluorescence and absorption spectra [28–30] show that the subnatural-linewidth effects, seen in the broadband squeezed vacuum case, are diminished and ultimately vanish when the bandwidth of the squeezed vacuum field is comparable to the natural linewidths of the atomic transitions.

The other important assumption in these calculations, which would limit experimental realization, was that the atoms exclusively interact with the squeezed modes. This could be difficult to realize experimentally, since it requires squeezing all the modes of the electromagnetic field coupled to the atoms. This situation would be realized in practice using some type of waveguide or generation of a squeezed perfect electric dipole wave [8]. In atomic spectroscopy, however, the experiments usually use atomic-beam methods [31], or atoms trapped in a confined space [32], where the atoms interact with an incoming wave which is not a perfect electric dipole. Schemes involving optical cavities with unsqueezed windows have been proposed as a possibility to avoid these difficulties [20,33,34].

In this paper we propose another scheme which involves three-level atoms strongly driven by two laser fields and coupled to a finite-bandwidth squeezed vacuum whose band-

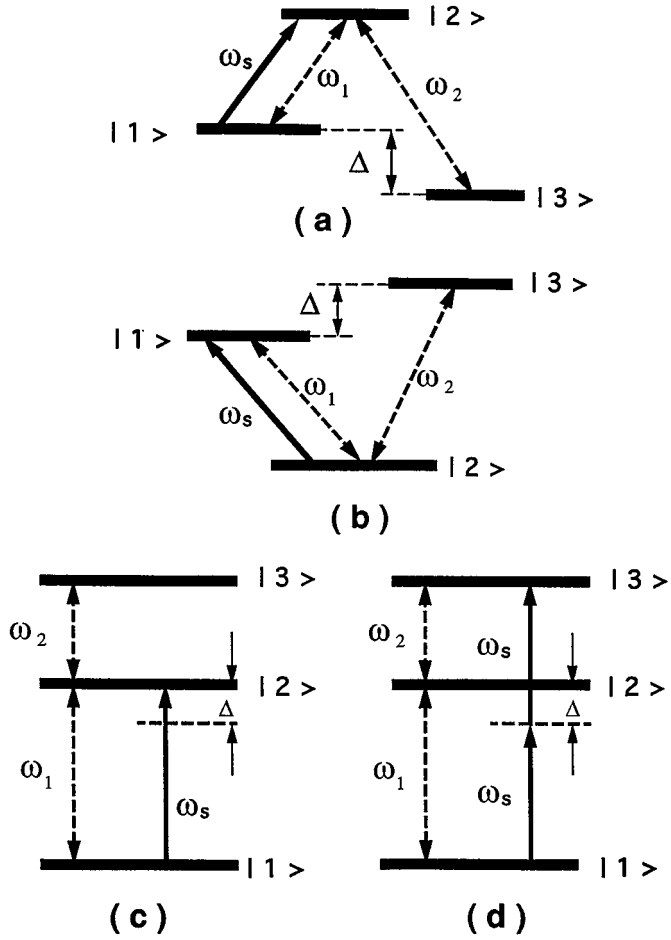

FIG. 1. Energy-level schemes for the four atomic configurations: (a) the Λ configuration, (b) the V configuration, (c) the cascade configuration with the squeezed vacuum coupled to the lower transition, and (d) the cascade configuration with the squeezed vacuum coupled to the two-photon transition.

width is much smaller than the difference in the allowed atomic transition frequencies. This scheme retains the advantage that the squeezed vacuum might be coupled to one of the two possible transitions and the fluorescence could be observed from the other transition whose frequency is well outside the squeezing bandwidth. This system might be regarded as a somewhat more practical scheme for observing the effects predicted in the fluorescence spectrum, as it does not require the experimentally difficult separation of the fluorescence field from the squeezed field.

We are particularly interested in the manner in which a narrow-band squeezed vacuum field coupled to one of the two atomic transitions affects the fluorescence field emitted from the other transition. Using master-equation techniques, we calculate the steady-state fluorescence spectra of the transition not coupled to the squeezed vacuum. We consider four three-level configurations shown in Fig. 1, i.e., lambda (Λ), vee (V), and cascade (Ξ), with the squeezed vacuum coupled to the lower transition, and a cascade with the squeezed vacuum coupled to the two-photon transition. We assume that the driving fields of Rabi frequencies Ω_1 and Ω_2 are each coupled to one of the atomic transitions, and their frequencies are exactly equal to the atomic transition frequencies ω_1 and ω_2, respectively. We find that in all these configurations the fluorescence spectra are strongly influenced by the squeezed vacuum field. In particular, for strongly driven Λ, V, and cascade systems with the squeezed vacuum coupled only to the transition of the frequency ω_1, the spectrum observed from the transition of frequency ω_2 consists of five lines with only those located at ω_2 and $\omega_2 \pm \Omega$ dependent on the squeezed vacuum phase φ_s, where $\Omega=(\Omega_1^2+\Omega_2^2)^{1/2}$ is the effective Rabi frequency of the driving fields. The lines at $\omega_2 \pm \frac{1}{2}\Omega$ do not show any dependence on φ_s. This is in contrast to the two-level atom case, where all spectral lines depend on the phase [20]. For a strongly driven cascade system with the squeezed vacuum field resonant with the two-photon transition between the ground and the most excited levels, all spectral lines show the dependence on the phase.

In order to explain these features, we apply the dressed-atom model [35]. In the limit of well-separated spectral lines (secular approximation), the master equation leads to separated equations for populations and coherences, which allows us to derive analytical expressions for the linewidths of the spectral features and their intensities. The dressed states of the systems are identified and the spectral features are explained in terms of transitions between these dressed states.

The paper is organized as follows. In Sec. II we present our model and discuss in detail the optical Bloch equations for the Λ configuration only. Calculations of the fluorescence spectra for all configurations are presented in Sec. III. The dressed-atom model of the system is discussed and the analytical expressions for the spectral linewidths and their intensities are derived in Sec. IV, again focusing only on the Λ configuration in the interests of conciseness. Finally, in Sec. V, we summarize our results.

II. THE MODEL

We consider three-level atoms with the nondegenerate states $|1\rangle$, $|2\rangle$, and $|3\rangle$ of energies E_1, E_2, and E_3 in the three possible configurations (Fig. 1)

$$\begin{aligned} &(1) \quad E_2>E_1>E_3, \quad \Lambda \text{ configuration} \\ &(2) \quad E_3>E_1>E_2, \quad \text{V configuration} \\ &(3) \quad E_3>E_2>E_1, \quad \Xi \text{ configuration.} \end{aligned} \tag{2.1}$$

The atoms interact with two single-mode coherent laser fields and with the quantized multimode radiation field in which a part of the modes is in a squeezed state. The first laser, of the Rabi frequency Ω_1, is coupled to the atomic transition $|1\rangle$–$|2\rangle$ and has a frequency ω_{1L} which is exactly equal to the atomic transition frequency ω_1, i.e., the one-photon detuning $\Delta_1=\omega_1-\omega_{1L}$ is zero. The second laser, of the Rabi frequency Ω_2, is coupled to the atomic transition $|3\rangle$–$|2\rangle$ and has a frequency ω_{2L} which is exactly equal to the atomic transition frequency ω_2, i.e., the one-photon detuning $\Delta_2=\omega_2-\omega_{2L}$ is zero. On the other hand, the frequency ω_{2L} is significantly different from ω_{1L}, so that each laser is coupled only to one of the two possible transitions in the three-level systems. We assume that a part of the vacuum modes coupled to the atom is in a multimode squeezed vacuum state. The bandwidth of squeezing is assumed to be much larger than the decay rates of the atomic transitions and the

Rabi frequencies of the driving fields. This allows the application of the Markoff approximation in terms of the free-atom states when calculating the fluorescence spectra.

The time evolution of the atomic systems is described by the master equation of the reduced density operator ρ. In the Schrödinger picture the master equation, based on the Born-Markoff approximations, is given by [36]

$$\begin{aligned}\frac{\partial\rho}{\partial t}=&-\frac{i}{\hbar}[H_0,\rho]-\frac{1}{2}\sum_{ij}\Gamma_{ij}[N(\omega_i)+1](S_i^+S_j^-\rho+\rho S_i^+S_j^-\\&-2S_j^-\rho S_i^+)-\frac{1}{2}\sum_{ij}\Gamma_{ij}N(\omega_i)(S_i^-S_j^+\rho+\rho S_i^-S_j^+\\&-2S_j^+\rho S_i^-)-\frac{1}{2}\sum_{ij}\Gamma_{ij}M(\omega_i)(S_i^+S_j^+\rho+\rho S_i^+S_j^+\\&-2S_j^+\rho S_i^+)e^{-2i\omega_s t}-\frac{1}{2}\sum_{ij}\Gamma_{ij}M^*(\omega_i)(S_i^-S_j^-\rho\\&+\rho S_i^-S_j^--2S_j^-\rho S_i^-)e^{2i\omega_s t},\end{aligned}\tag{2.2}$$

where S_i^+ (S_i^-) is the raising (lowering) atomic operator of the ith transition ($i=1,2$), H_0 is the Hamiltonian composed of two terms

$$H_0=H_{Al}+W_l,\tag{2.3}$$

where H_{Al} is the Hamiltonian of the atom in the lth configuration ($l=\Lambda,\mathrm{V},\Xi$), and

$$\begin{aligned}W_l=&\tfrac{1}{2}\hbar\Omega_1[S_1^+\exp(-i\omega_1 t)+S_1^-\exp(i\omega_1 t)]\\&+\tfrac{1}{2}\hbar\Omega_2[S_2^+\exp(-i\omega_2 t)+S_2^-\exp(i\omega_2 t)]\end{aligned}\tag{2.4}$$

is the interaction between the atom and the driving laser fields. In Eq. (2.4), we have assumed that the Rabi frequencies Ω_1 and Ω_2 are real and, for simplicity, we have set the laser phases to zero. The atomic operators $S_i^{\pm}$ and the Hamiltonian H_0 appearing in Eqs. (2.2)–(2.4) depend on the configuration of the atomic levels.

The parameters Γ_{ii}, which appear in Eq. (2.2), are the decay rates for the ith transition and Γ_{ij} ($i\neq j$) are the coherence transfer rates. Explicit expressions are given in [36]. The parameters $N(\omega_i)$ and $M(\omega_i)=|M(\omega_i)|\exp(i\varphi_s)$ characterize a squeezed vacuum field of carrier frequency ω_s and phase φ_s. The explicit form of the squeezing parameters depends on the specific process used in the generation of the squeezed vacuum field. Present sources of squeezed light are degenerate or nondegenerate parametric amplifiers. We first consider a squeezed vacuum field which is the output of a degenerate parametric amplifier (DPA). In practice, this has proved to be the most successful source of squeezed light [37]. In this case [38],

$$N(\omega_i)=\frac{b_y^2-b_x^2}{4}\left[\frac{1}{(\omega_s-\omega_i)^2+b_x^2}-\frac{1}{(\omega_s-\omega_i)^2+b_y^2}\right],\tag{2.5}$$

$$|M(\omega_i)|=\frac{b_y^2-b_x^2}{4}\left[\frac{1}{(\omega_s-\omega_i)^2+b_x^2}+\frac{1}{(\omega_s-\omega_i)^2+b_y^2}\right],\tag{2.6}$$

with

$$b_x=\tfrac{1}{2}\gamma-|\mathcal{E}|,\quad b_y=\tfrac{1}{2}\gamma+|\mathcal{E}|,\tag{2.7}$$

where γ is the DPA cavity damping rate and $\mathcal{E}$ is the effective pump intensity [38]. Maximum squeezing is achieved at the threshold for parametric oscillation, i.e., as $|\mathcal{E}|\rightarrow\frac{1}{2}\gamma$. The parameters b_x and b_y are referred to as the bandwidths of the squeezed vacuum field.

It is seen from Eqs. (2.5) and (2.6) that the squeezing parameters depend on the detuning between the carrier frequency of the squeezed field and the atomic transition frequencies. For the squeezed-field frequency ω_s centered on the atomic transition frequency ω_1, the squeezing parameters take the form

$$\begin{aligned}N(\omega_1)&=\frac{b_y^2-b_x^2}{4}\left(\frac{1}{b_x^2}-\frac{1}{b_y^2}\right)=N,\\|M(\omega_1)|&=\frac{b_y^2-b_x^2}{4}\left(\frac{1}{b_x^2}+\frac{1}{b_y^2}\right)=|M|,\\N(\omega_2)&=\frac{b_y^2-b_x^2}{4}\left[\frac{1}{\Delta^2+b_x^2}-\frac{1}{\Delta^2+b_y^2}\right],\\|M(\omega_2)|&=\frac{b_y^2-b_x^2}{4}\left[\frac{1}{\Delta^2+b_x^2}+\frac{1}{\Delta^2+b_y^2}\right],\end{aligned}\tag{2.8}$$

where $\Delta=\omega_1-\omega_2$ is the frequency difference between the two atomic transitions. When Δ is much larger than the bandwidth of the squeezed vacuum ($\Delta\gg b_x,b_y$), the transition $|2\rangle-|3\rangle$ is decoupled from the squeezed vacuum field. In this case it is possible to observe the fluorescence field on the $|2\rangle-|3\rangle$ transition without applying experimentally difficult techniques of separating the fluorescence field from the squeezed vacuum field.

For the Λ *configuration*, with the energies of the atomic levels related as $E_2>E_1>E_3$, the atomic operators $S_i^{\pm}$ are given by

$$\begin{aligned}S_1^+&=(S_1^-)^\dagger=|2\rangle\langle 1|,\\S_2^+&=(S_2^-)^\dagger=|2\rangle\langle 3|,\end{aligned}\tag{2.9}$$

and the Hamiltonian $H_{A\Lambda}$ for the Λ-type three-level atom is given by

$$H_{A\Lambda}=\hbar[\omega_2|2\rangle\langle 2|+(\omega_2-\omega_1)|1\rangle\langle 1|].\tag{2.10}$$

where we have assumed that $E_3=0$.

The dynamics of the Λ-type atom interacting with a squeezed vacuum field and driven by two coherent laser fields is governed by the optical Bloch equations for the density matrix elements. In order to study the spectral properties of the fluorescence field not superimposed on the squeezed vacuum field, we suppose that the carrier frequency of the squeezed field $\omega_s=\omega_1$ and $\Delta\gg b_x,b_y$. The master equation (2.2) with (2.3), (2.4), (2.9), (2.10), and the squeezing parameters (2.8) leads to the following optical Bloch equations for the density matrix elements:

$$\dot{\tilde{\rho}}_{11}=-N\gamma_1\tilde{\rho}_{11}+(N+1)\gamma_1\tilde{\rho}_{22}+\tfrac{1}{2}\xi_1(\tilde{\rho}_{12}+\tilde{\rho}_{21}),$$

$$\dot{\tilde{\rho}}_{22}=-[(N+1)\gamma_1+\gamma_2]\tilde{\rho}_{22}+N\gamma_1\tilde{\rho}_{11}-\tfrac{1}{2}\xi_1(\tilde{\rho}_{12}+\tilde{\rho}_{21})+\tfrac{1}{2}\xi_2(\tilde{\rho}_{23}+\tilde{\rho}_{32}),$$

$$\dot{\tilde{\rho}}_{12}=(\dot{\tilde{\rho}}_{21})^*=-\tfrac{1}{2}[(2N+1)\gamma_1+\gamma_2]\tilde{\rho}_{12}-M^*\gamma_1\tilde{\rho}_{21}-\tfrac{1}{2}\xi_2\tilde{\rho}_{13}-\tfrac{1}{2}\xi_1(\tilde{\rho}_{11}-\tilde{\rho}_{22}), \tag{2.11}$$

$$\dot{\tilde{\rho}}_{32}=(\dot{\tilde{\rho}}_{23})^*=-\tfrac{1}{2}[(N+1)\gamma_1+\gamma_2]\tilde{\rho}_{32}-\tfrac{1}{2}\xi_1\tilde{\rho}_{31}+\tfrac{1}{2}\xi_2(\tilde{\rho}_{11}+2\tilde{\rho}_{22})-\tfrac{1}{2}\xi_2,$$

$$\dot{\tilde{\rho}}_{13}=(\dot{\tilde{\rho}}_{31})^*=-\tfrac{1}{2}N\gamma_1\tilde{\rho}_{13}+\tfrac{1}{2}\xi_2\tilde{\rho}_{12}+\tfrac{1}{2}\xi_1\tilde{\rho}_{23},$$

where the overdot denotes differentiation with respect to $(\Gamma_{11}+\Gamma_{22})t$,

$$\tilde{\rho}_{12}=(\tilde{\rho}_{21})^*=i\rho_{12}\exp(-i\omega_1 t),$$

$$\tilde{\rho}_{32}=(\tilde{\rho}_{23})^*=i\rho_{32}\exp(-i\omega_2 t),$$

$$\tilde{\rho}_{13}=(\tilde{\rho}_{31})^*=\rho_{13}\exp[-i(\omega_1-\omega_2)t] \tag{2.12}$$

are the slowly varying parts of the off-diagonal matrix elements, and

$$\gamma_1=\frac{\Gamma_{11}}{\Gamma_{11}+\Gamma_{22}},\quad \gamma_2=\frac{\Gamma_{22}}{\Gamma_{11}+\Gamma_{22}},\qquad \xi_1=\frac{\Omega_1}{\Gamma_{11}+\Gamma_{22}},\quad \xi_2=\frac{\Omega_2}{\Gamma_{11}+\Gamma_{22}}, \tag{2.13}$$

are dimensionless parameters for the atomic decay rates γ_1 and γ_2 in the normal vacuum $[\Gamma_{ii}\equiv\Gamma_{ii}^{+}(N=0)]$, and the Rabi frequencies ξ_1 and ξ_2 of the driving fields.

The derivation of the optical Bloch equations for the V and cascade systems follows the same procedure as that used for the Λ system. For the Λ and V systems the coherence transfer rates Γ_{ij} $(i\neq j)$ do not appear as the time dependence of the terms with which they are associated includes an oscillation at the frequency difference Δ. For the cascade system, however, the coherence transfer rates do make an appearance when the atom is coupled to a nondegenerate parametric amplifier whose output properties are given in [39].

In the next section, the optical Bloch equations such as (2.11) will be used in our calculations of the spectral properties of the fluorescence field emitted from the transition $|2\rangle$-$|3\rangle$ of the Λ, V, and cascade systems.

III. FLUORESCENCE SPECTRA

The incoherent steady-state spectrum of the fluorescence field emitted from a three-level atom is defined as the Fourier transform of the two-time correlation function of the atomic dipole operators:

$$S(\omega)=\mathrm{Re}\sum_{i=1}^{2}\int_0^\infty d\tau\, e^{i\omega\tau}\lim_{t\to\infty}[\langle S_i^+(t)S_j^-(t+\tau)\rangle-\langle S_i^+(t)\rangle\times\langle S_j^-(t+\tau)\rangle]. \tag{3.1}$$

For well-separated atomic transition frequencies $(\Delta\gg\Gamma_{ij})$, the spectrum (3.1) can be written as a sum of two independent terms:

$$S(\omega)=\mathrm{Re}\int_0^\infty d\tau\{\lim_{t\to\infty}[\langle\tilde{S}_1^+(t)\tilde{S}_1^-(t+\tau)\rangle-\langle\tilde{S}_1^+(t)\rangle\langle\tilde{S}_1^-(t+\tau)\rangle]\exp[i(\omega-\omega_{1L})\tau]+\lim_{t\to\infty}[\langle\tilde{S}_2^+(t)\tilde{S}_2^-(t+\tau)\rangle-\langle\tilde{S}_2^+(t)\rangle\langle\tilde{S}_2^-(t+\tau)\rangle]\times\exp[i(\omega-\omega_{2L})\tau]\}, \tag{3.2}$$

where

$$\tilde{S}_i^{\pm}(t)=S_i^{\pm}(t)\exp(\mp i\omega_{iL}t),\quad i=1,2 \tag{3.3}$$

are the slowly varying parts of the atomic operators.

The first term on the right-hand side of (3.2) will differ significantly from zero only for those frequencies ω which are near the laser frequency ω_{1L}. Similarly, the second term differs significantly from zero only for those frequencies ω which are near the laser frequency ω_{2L}. Therefore, the incoherent spectrum of the fluorescence field emitted with frequencies ω near the frequency ω_2 of the $|2\rangle$-$|3\rangle$ transition driven by the laser of frequency ω_{2L} is given by

$$S_2(\omega)=\mathrm{Re}\int_0^\infty d\tau\, e^{i(\omega-\omega_{2L})\tau}G(\tau), \tag{3.4}$$

where

$$G(\tau)=\lim_{t\to\infty}[\langle\tilde{S}_2^+(t)\tilde{S}_2^-(t+\tau)\rangle-\langle\tilde{S}_2^+(t)\rangle\langle\tilde{S}_2^-(t+\tau)\rangle]. \tag{3.5}$$

Introducing the Laplace transform, we express the incoherent fluorescence spectrum in the form

$$S_{\mathrm{in}}(\omega)=\mathrm{Re}G(z)\big|_{z=-i\nu}, \tag{3.6}$$

where $\nu=(\omega-\omega_{2L})/(\Gamma_{11}+\Gamma_{22})$, and $G(z)$ denotes the Laplace transform of the atomic correlation function $G(\tau)$. In order to calculate the incoherent fluorescence spectrum we have to compute the Laplace transform $G(z)$ of the atomic correlation function $G(\tau)$. From the quantum regression theorem [40], it is well known that for $\tau>0$ the two-time average $\langle\tilde{S}_2^+(t)\tilde{S}_2^-(t+\tau)\rangle$ satisfies the same equation of motion as the one-time average $\langle\tilde{S}_2^-(\tau)\rangle$. On the other hand, the average $\langle\tilde{S}_2^-(\tau)\rangle$ satisfies the same equation of motion as the density matrix element $\tilde{\rho}_{23}(\tau)$. The Laplace transforms of the density matrix elements are readily obtained from the Bloch equations of motion, such as (2.11).

From the optical Bloch equations (2.11), we find that the set of equations for the Laplace transforms of the two-time correlation functions can be written in a matrix form as

$$L(z)\vec{X}(z)=\vec{X}(0), \tag{3.7}$$

where $\vec{X}(z)$ is a column vector composed of the Laplace transforms of the steady-state values of the atomic correlation functions, $\vec{X}(0)$ is a column vector of the initial values of the transformed atomic correlation functions, and $L(z)$ is an

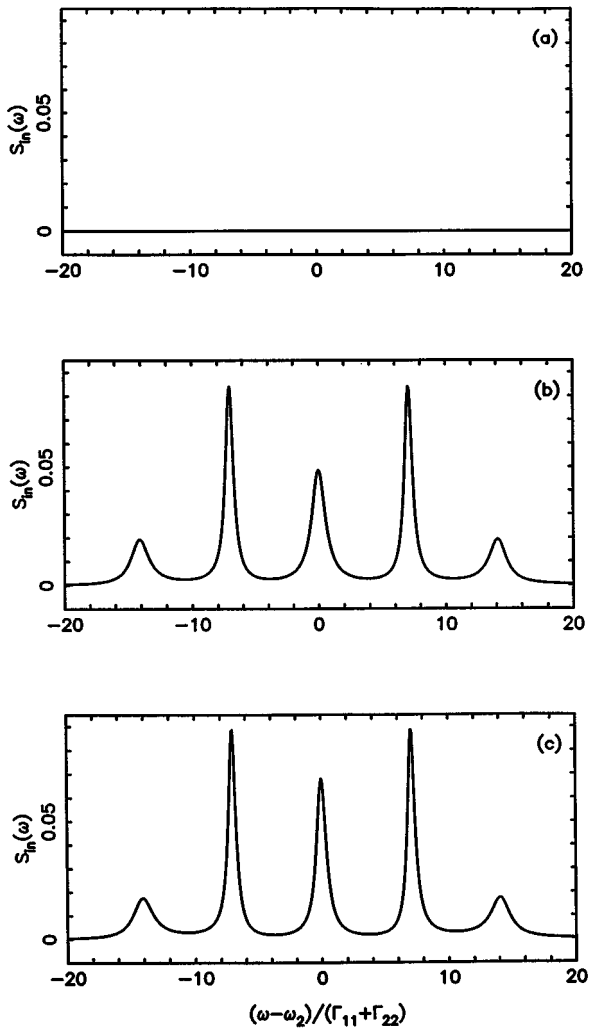

FIG. 2. The incoherent fluorescence spectra for the Λ configuration with $\gamma_1=\gamma_2=0.5$, $\xi_1=\xi_2=10$, and different vacua: (a) the ordinary vacuum ($N=|M|=0$), (b) thermal vacuum field ($N=0.4$, $|M|=0$), and (c) squeezed vacuum [$N=0.4$, $|M|^2=N(N+1)$, $\varphi_s=0$].

8×8 matrix obtained from the coefficients appearing in the optical Bloch equations of the density matrix elements.

The incoherent fluorescence spectrum is shown in Fig. 2 for $\xi_1=\xi_2=10$, $\gamma_1=\gamma_2=0.5$, and different vacua. For the ordinary vacuum, $N=|M|=0$, and the spectrum vanishes [Fig. 2(a)], indicating that there is no fluorescence emitted from the Λ system. The lack of fluorescence is due to the coherent population trapping effect [41–43], which prevents fluorescence from the Λ system when the driving fields are on the two-photon resonance with the atomic transitions. For a thermal vacuum field [Fig. 2(b)], $N\neq 0$, $|M|=0$, and a nonzero spectrum appears composed of five lines, one located at the central frequency $\omega=\omega_2$ and two pairs of sidebands located at $\omega=\omega_2\pm\frac{1}{2}\Omega$ and $\omega=\omega_2\pm\Omega$, where $\Omega=(\Omega_1^2+\Omega_2^2)^{1/2}$ is the effective Rabi frequency of the two driving fields. The appearance of the fluorescence field in a thermal vacuum field results from thermal fluctuations which destroy the coherent population trapping effect [36]. When the transition $|2\rangle$-$|1\rangle$ is coupled to a squeezed vacuum field [Fig. 2(c)], the spectrum shows five lines which have the same positions as their counterparts in the thermal field, but some of them have widely

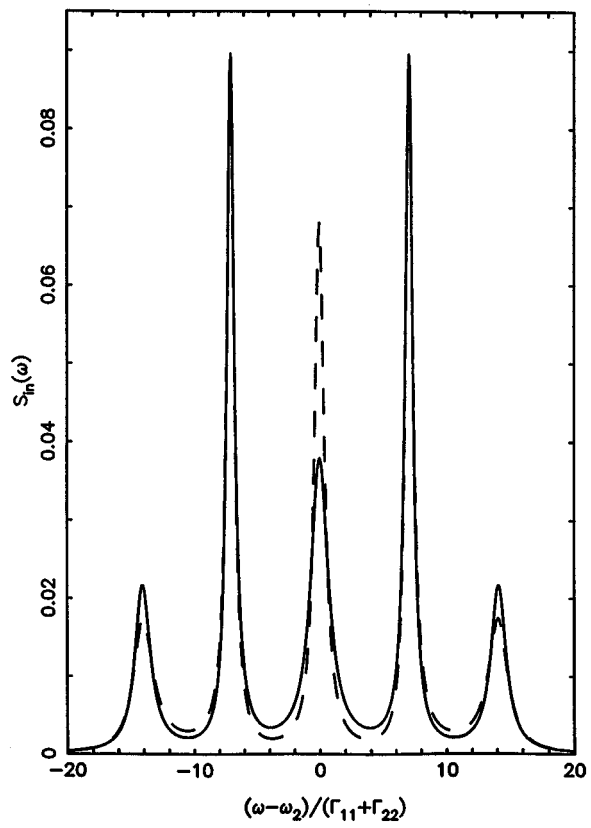

FIG. 3. The incoherent fluorescence spectrum for the Λ configuration with $\gamma_1=\gamma_2=0.5$, $\xi_1=\xi_2=10$ squeezed vacuum coupled to the $|2\rangle$-$|1\rangle$ transition, and different phases: $\varphi_s=0$ (solid line) and $\varphi_s=\pi$ (dashed line). The squeezing parameters are $N=0.4$, $|M|^2=N(N+1)$.

differing intensities and widths. In fact, the central line and the outer sidebands depend on the phase of the squeezed vacuum, whereas the inner sidebands are completely independent of the phase. This is shown in Fig. 3, where we plot the spectrum for the same parameters as in Fig. 2(c), but for different phases φ_s. It is evident from Fig. 3 that only the central line and the outer sidebands depend on the phase, whereas the inner sidebands are completely independent of the phase. We explain these features in terms of the dressed-atom model of the system, which will be discussed in Sec. IV.

The same procedure as the above is used to calculate the fluorescence spectrum for the V *system*. In Fig. 4 we plot the fluorescence spectrum for the V configuration with $\xi_1=\xi_2=10$, $\gamma_1=\gamma_2=0.5$, and different vacua. For the ordinary vacuum ($N=|M|=0$) the spectrum exhibits three lines, the central line located at $\omega=\omega_2$ and two sidebands at $\omega=\omega_2\pm\Omega$. The spectrum is similar to the well-known Mollow triplet [44] of a two-level atom driven by a strong laser field. When the transition $|2\rangle$-$|1\rangle$ is coupled to a thermal vacuum field [Fig. 4(b)], additional sidebands appear in the spectrum located at $\omega=\omega_2\pm\frac{1}{2}\Omega$. The lack of these lines in the ordinary vacuum results from the trapping of the atomic population in a linear superposition of the upper levels and the ground $|2\rangle$ level, which effectively reduces the system to two levels [45,46]. The thermal fluctuations destroy this trapping and additional sidebands appear in the spectrum. When

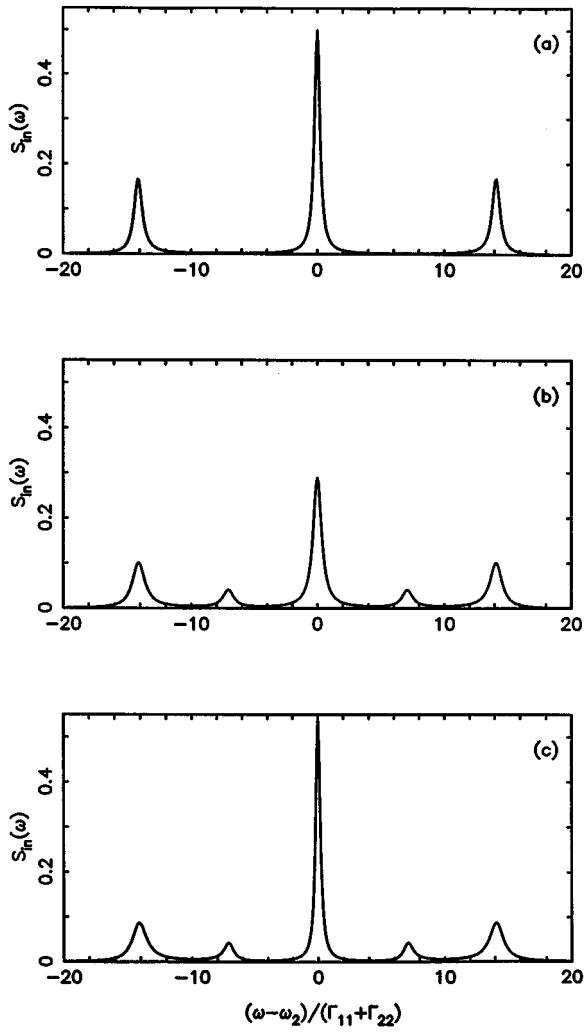

FIG. 4. The incoherent fluorescence spectrum for the V configuration with $\gamma_1=\gamma_2=0.5$, $\xi_1=\xi_2=10$, and different vacua: (a) the ordinary vacuum ($N=|M|=0$), (b) thermal vacuum field ($N=0.4$, $|M|=0$), and (c) squeezed vacuum [$N=0.4$, $|M|^2=N(N+1)$, $\varphi_s=0$].

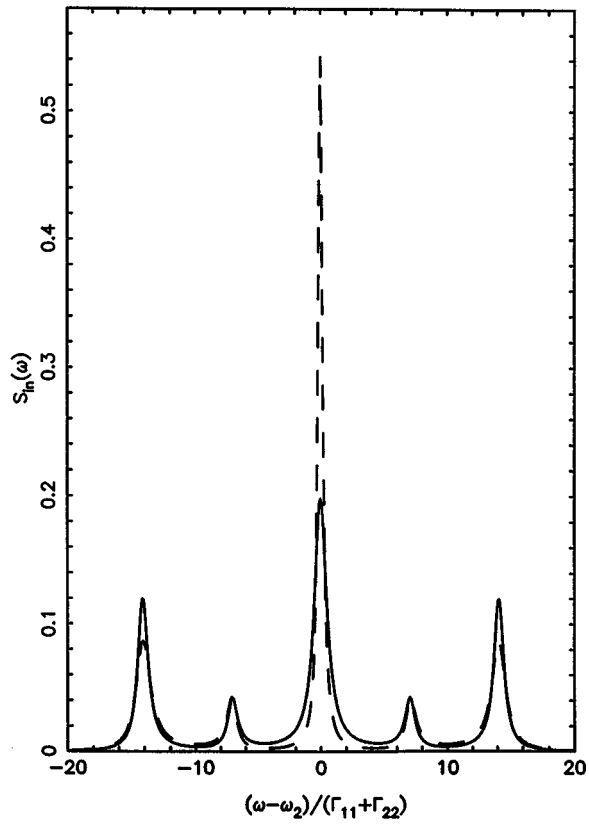

FIG. 5. The incoherent fluorescence spectrum for the V configuration with $\gamma_1=\gamma_2=0.5$, $\xi_1=\xi_2=10$ squeezed vacuum coupled to the $|2\rangle$-$|1\rangle$ transition, and different phases: $\varphi_s=0$ (solid line) and $\varphi_s=\pi$ (dashed line). The squeezing parameters are $N=0.4$, $|M|^2=N(N+1)$.

the $|2\rangle$-$|1\rangle$ transition is coupled to a squeezed vacuum field [Fig. 4(c)], the spectrum shows five lines but their intensities and widths differ from those found in the thermal field. In Fig. 5, we plot the spectrum for the same parameters as in Fig. 4(c), but for different phases. We see that the spectrum, similar to that of the Λ configuration, exhibits five lines with only the central line and the outer sidebands dependent on the squeezing phase.

For the *cascade configuration*, we consider first the incoherent spectrum of the fluorescence field emitted on the $|3\rangle$-$|2\rangle$ transition with the carrier frequency of the squeezed vacuum equal to the frequency of the lower $|2\rangle$-$|1\rangle$ transition, and the squeezed vacuum field taken to be the output of a degenerate parametric amplifier. In this case, we assume that the squeezing bandwidth is much smaller than the frequency difference Δ, so that the squeezed vacuum is exclusively coupled to the $|2\rangle$-$|1\rangle$ transition. In the second case, the carrier frequency of the squeezed vacuum is made equal to the average frequency of the two atomic transitions, and we assume that the squeezed vacuum is the output of a nondegenerate parametric amplifier with the two spectral peaks centered on the transition frequencies ω_1 and ω_2. In both cases, the spectrum can be calculated via the same procedure as used for the Λ system.

In the first case, the spectrum is plotted in Fig. 6 for $\xi_1=\xi_2=10$, $\gamma_1=\gamma_2=0.5$, and different vacua. In all cases the spectrum exhibits five lines located at $\omega=\omega_2,\omega_2\pm\frac{1}{2}\Omega$, and $\omega_2\pm\Omega$, in agreement with the fluorescent spectrum obtained by Whitley and Stroud [47]. Their intensities and widths, however, depend on the squeezed parameters N and M, with only the central component and the outer sidebands dependent on the phase φ_s. This is shown in Fig. 7, where we plot the fluorescence spectrum for the same parameters as in Fig. 6(c), but for different phases. The phase dependence is similar to that found for the Λ and V configurations with only the central line and the outer sidebands dependent on the squeezing phase. A similar phase dependence of the spectral features has been found by Jagatap, Lawande, and Lawande [26], who calculated the fluorescence spectrum for a cascade three-level atom coupled to two independent squeezed vacua.

In the second case we take into account the coupling of a nondegenerate parametric amplifier to the cascade atom, which alters the form of the optical Bloch equations in a fashion described at the end of Sec. II. We plot the spectrum in Fig. 8 for $\xi_1=\xi_2=10$, $\gamma_1=\gamma_2=\gamma_c=0.5$, $N=0.4$, $|M|^2=N(N+1)$, and different phases φ_s. Figure 8 demonstrates the important feature that now all spectral lines depend on the squeezing phase, with the central line and the

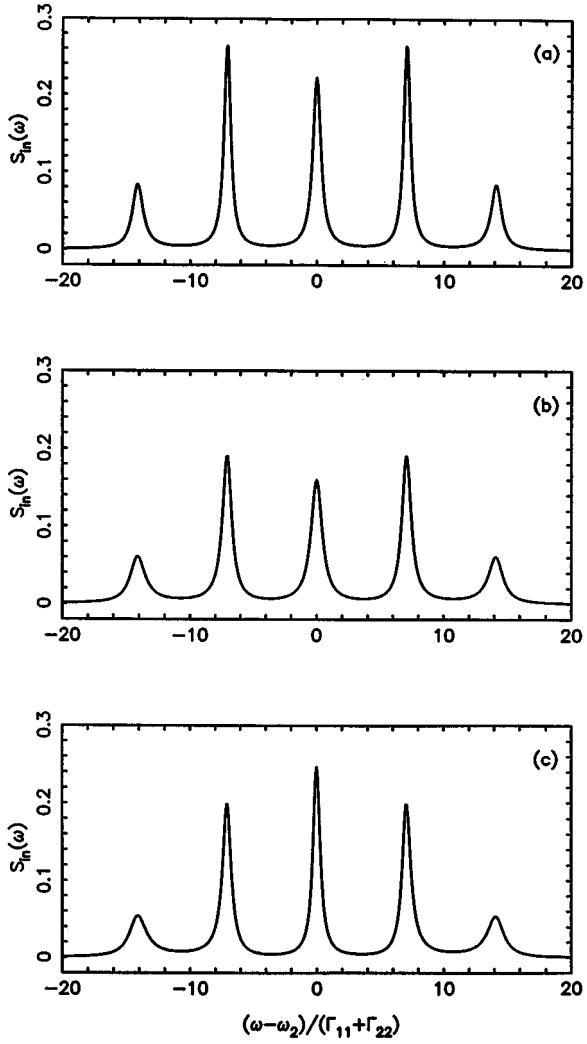

FIG. 6. The incoherent fluorescence spectrum for the cascade configuration with $\gamma_1=\gamma_2=0.5$, $\xi_1=\xi_2=10$, and different vacua: (a) the ordinary vacuum ($N=|M|=0$), (b) thermal vacuum field ($N=0.4$, $|M|=0$), and (c) squeezed vacuum coupled to the $|2\rangle$-$|1\rangle$ transition [$N=0.4$, $|M|^2=N(N+1)$, $\varphi_s=0$].

outer sidebands exhibiting the same variation between narrowing and broadening. A nonzero value for the coherence transfer rate $\gamma_c=\Gamma_{12}/(\Gamma_{11}+\Gamma_{22})$ is essential in observing the phase dependence of the spectral features.

IV. DRESSED-ATOM MODEL EXPLANATION OF THE SPECTRAL FEATURES

In Sec. III graphical results for the incoherent fluorescence spectra for the three possible configurations of a three-level system were presented. Here, we give a dressed-atom model explanation of the spectral features in terms of the energy levels of the dressed states and transitions among these states. We perform the calculations using the dressed-atom technique developed by Cohen-Tannoudji and Reynaud [35]. In this model the driving laser fields are treated quantum mechanically and the eigenstates of the combined atom and driving-field system are found and used as the basis for further calculations. We consider only the Λ configuration as the V and cascade configurations follow the same method.

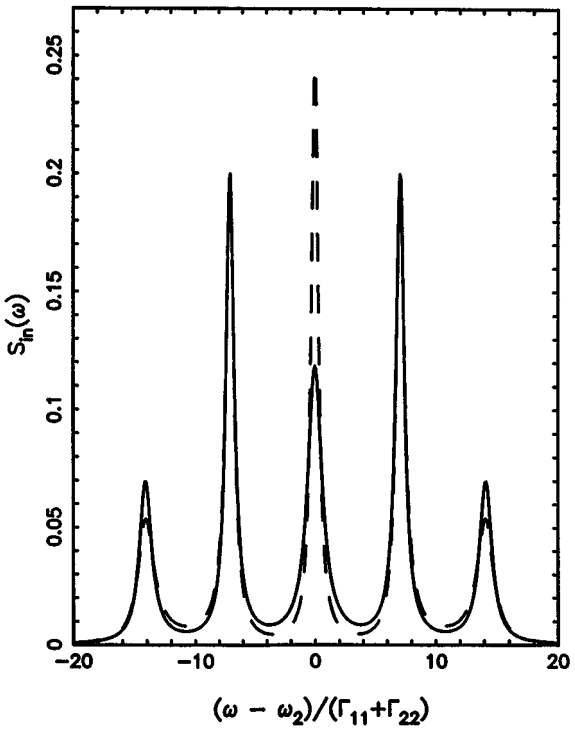

FIG. 7. The incoherent fluorescence spectrum for the cascade configuration with $\gamma_1=\gamma_2=0.5$, $\xi_1=\xi_2=10$ squeezed vacuum coupled to the $|2\rangle$-$|1\rangle$ transition, and different phases: $\varphi_s=0$ (solid line) and $\varphi_s=\pi$ (dashed line). The squeezing parameters are $N=0.4$, $|M|^2=N(N+1)$.

The method is essentially based on the original master equation (2.2) though with the unperturbed Hamiltonian H_0 modified to include the free-field Hamiltonian for the laser driving fields and the atom-field interaction (2.4) replaced by a fully quantum coupling. The original Markovian relaxation terms in (2.2) based on free-atom states are still valid in the present finite-bandwidth squeezed-vacuum case, since the squeezed-vacuum bandwidths (which determine the reservoir correlation time) are large compared to the Rabi frequency. Master equations for the system density matrix elements in a dressed-atom basis can be obtained via the unitary matrix that relates the dressed-atom basis states to the uncoupled basis states. For convenience, we will write $n=n_1+n_2$ as the total number of photons in the laser fields and $q=n_1-n_2$ as the photon-number difference. The uncoupled state $|i,n_1,n_2\rangle$ is given by $|i\rangle\otimes|n_1\rangle\otimes|n_2\rangle$. The dressed-atom states will be designated $|i,n,q\rangle$. To determine the fluorescence field associated with the $|2\rangle$-$|3\rangle$ transition we will require the populations P_{inq} of the dressed states and the coherences $\rho^{(+)}_{ij,nq}$ between dressed states $|i,n,q\rangle$ and $|j,n-1,q+1\rangle$. In terms of density matrix elements these are given by

$$P_{inq}=\langle i,n,q|\rho|i,n,q\rangle, \tag{4.1}$$

$$\rho^{(+)}_{ij,nq}=\langle i,n,q|\rho|j,n-1,q+1\rangle. \tag{4.2}$$

The Hamiltonian for the atom in a Λ *configuration* and interacting with the quantized driving fields may be written as

$$H=H_{AF}+W_L', \tag{4.3}$$

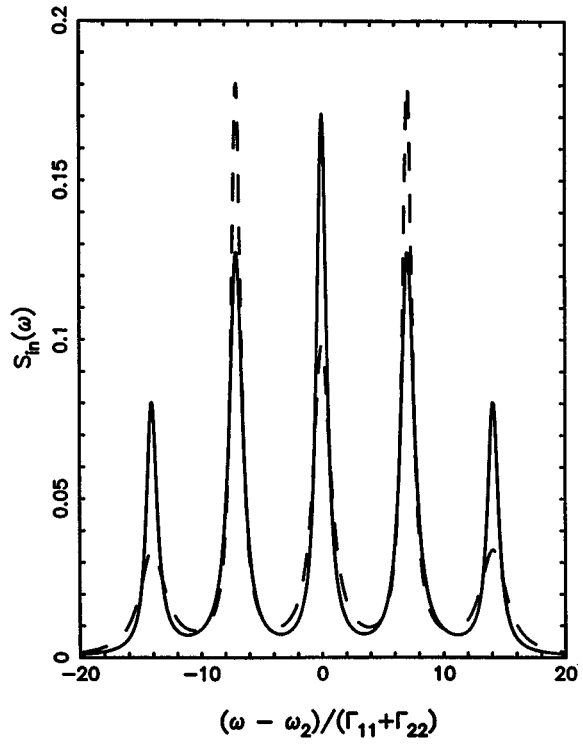

FIG. 8. The incoherent fluorescence spectrum for the cascade configuration with $\gamma_1=\gamma_2=\gamma_c=0.5$, $\xi_1=\xi_2=10$ squeezed vacuum coupled to the two-photon transition $|3\rangle$-$|1\rangle$, and different phases: $\varphi_s=0$ (solid line) and $\varphi_s=\pi$ (dashed line). The squeezing parameters are $N=0.4$ and $|M|^2=N(N+1)$.

where

$$H_{AF}=\hbar[\omega_2|2\rangle\langle 2|+(\omega_2-\omega_1)|1\rangle\langle 1|]+\hbar\omega_1 a_1^\dagger a_1 + \hbar\omega_2 a_2^\dagger a_2 \tag{4.4}$$

is the unperturbed (noninteracting) Hamiltonian of the atom plus driving laser fields of frequencies ω_1 and ω_2, and

$$W_L'=\tfrac{1}{2}i\hbar g_1(S_1^+ a_1-a_1^\dagger S_1^-)+\tfrac{1}{2}i\hbar g_2(S_2^+ a_2-a_2^\dagger S_2^-) \tag{4.5}$$

is the interaction Hamiltonian for the atom and the driving fields. In Eqs. (4.4) and (4.5), a_1 (a_2) and $a_1^\dagger$ ($a_2^\dagger$) are the annihilation and creation operators for the driving field of frequency ω_1 (ω_2) and g_1 and g_2 are the coupling constants between the atom and the driving fields. We assume that the driving fields of frequencies ω_1 and ω_2 are single-mode laser fields in the coherent states $|\alpha_1\rangle$ and $|\alpha_2\rangle$, respectively, where $\overline{n}_1=|\alpha_1|^2\gg 1$ is the mean number of photons in the mode of frequency ω_1, while $\overline{n}_2=|\alpha_2|^2\gg 1$ is the mean number of photons in the mode of frequency ω_2. The phases of α_1 and α_2 are taken to be zero in accordance with the theory of Sec. II. Such coherent states have associated classical fields which correspond to the semiclassical coupling (2.4).

The eigenstates (undressed states) of the noninteracting Hamiltonian H_{AF} form manifolds [see Fig. 9(a)] composed of threefold-degenerate states $|2,n_1,n_2\rangle$, $|1,n_1+1,n_2\rangle$, and $|3,n_1,n_2+1\rangle$ of energy

$$E_{nq}=\hbar[n_1\omega_1+(n_2+1)\omega_2]. \tag{4.6}$$

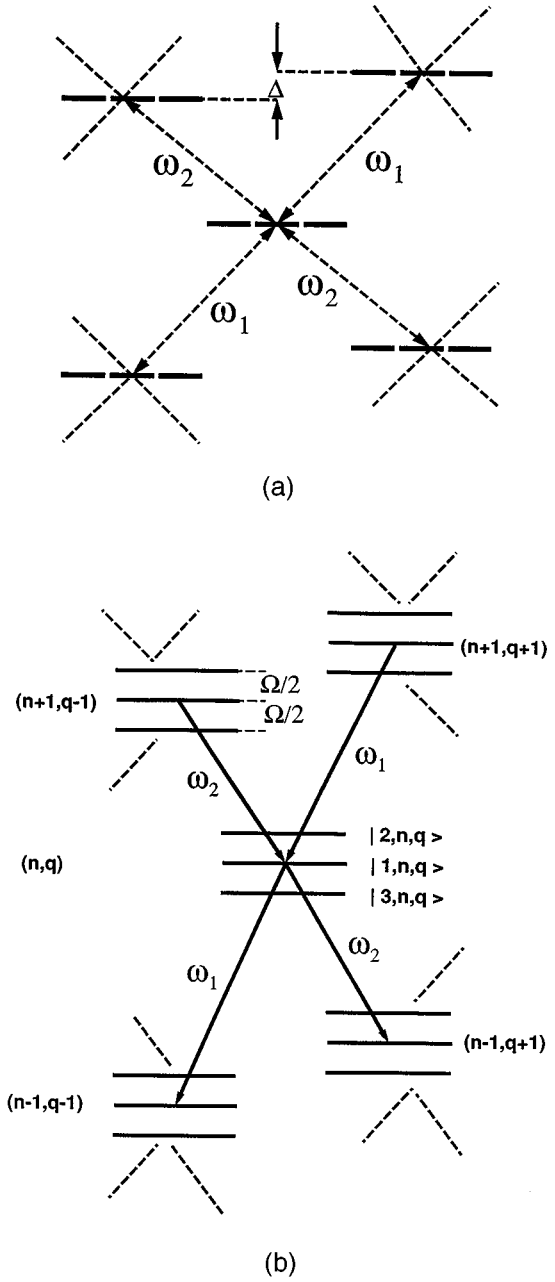

FIG. 9. Energy-level diagrams of the undressed Hamiltonian (a) and the dressed system (b). The manifold (n,q) is separated from the manifolds $(n\mp 1,q\pm 1)$ by the frequency ω_2, and from the manifolds $(n\pm 1,q\pm 1)$ by the frequency ω_1.

When we include the interaction W_L', the degeneracy is lifted, resulting in an energy-level scheme consisting of triplets [see Fig. 9(b)]. The dressed states in the set (n,q) are given by

$$|1,n,q\rangle=\frac{1}{\Omega}(-\Omega_2|1,n_1+1,n_2\rangle+\Omega_1|3,n_1,n_2+1\rangle),$$

$$|2,n,q\rangle=\frac{1}{\sqrt{2}\Omega}(\Omega_1|1,n_1+1,n_2\rangle+i\Omega|2,n_1,n_2\rangle + \Omega_2|3,n_1,n_2+1\rangle), \tag{4.7}$$

$$|3,n,q\rangle=\frac{1}{\sqrt{2}\Omega}\,(\Omega_1|1,n_1+1,n_2\rangle-i\Omega|2,n_1,n_2\rangle$$
$$+\Omega_2|3,n_1,n_2+1\rangle),$$

with energies

$$E_{1nq}=E_{nq},$$
$$E_{2nq}=E_{nq}+\tfrac{1}{2}\hbar\Omega, \tag{4.8}$$
$$E_{3nq}=E_{nq}-\tfrac{1}{2}\hbar\Omega,$$

where $\Omega=(\Omega_1^2+\Omega_2^2)^{1/2}$ with $\Omega_1=g_1(\bar{n}_1)^{1/2}$ and $\Omega_2=g_2(\bar{n}_2)^{1/2}$, and we have assumed the driving fields to be sufficiently intense that the variation of n-photon Rabi frequencies with n_1 and n_2 has been neglected and the photon numbers replaced by the average numbers of photons $\bar{n}_1$ and $\bar{n}_2$ in the laser modes.

Having available the dressed states of the system, we can set up master equations for the populations of the dressed states $|i,n,q\rangle$ and for coherences between dressed-atom states in the $|i,n,q\rangle$ and $|i,n-1,q+1\rangle$ sets. Coherences between $|i,n,q\rangle$ and $|i,n-1,q+1\rangle$ are not required, since we are interested in the spectral properties of the fluorescence field emitted at the $|2\rangle$-$|3\rangle$ transition, thereby limiting our calculations to the transitions between the dressed states of two neighboring manifolds separated by the frequency ω_2.

Considering only the energy diagram, Fig. 9(b), it is apparent that the possibility of fluorescence exists at five different frequencies,

$$\omega_{ij}=\hbar^{-1}(E_{inq}-E_{jn-1q+1}), \tag{4.9}$$

given by

$$\omega_{11}=\omega_{22}=\omega_{33}=\omega_2,$$
$$\omega_{12}=\omega_{31}=\omega_2-\tfrac{1}{2}\Omega,$$
$$\omega_{21}=\omega_{13}=\omega_2+\tfrac{1}{2}\Omega, \tag{4.10}$$
$$\omega_{23}=\omega_2+\Omega,$$
$$\omega_{32}=\omega_2-\Omega.$$

These frequencies exactly correspond to the frequencies of the spectral lines presented in Fig. 2.

Transitions from the manifold (n,q) to the manifolds $(n-1,q-1)$ and $(n-1,q+1)$ occur with probabilities given via the Fermi golden rule from first-order perturbation theory as

$$\gamma_{ij}=\Gamma_{11}|\langle i,n,q|S_1^+|j,n-1,q-1\rangle|^2$$
$$+\Gamma_{22}|\langle i,n,q|S_2^+|j,n-1,q+1\rangle|^2. \tag{4.11}$$

Using Eqs. (4.7) the probabilities (4.11) are given by

$$\gamma_{11}=\gamma_{12}=\gamma_{13}=0,$$
$$\gamma_{22}=\gamma_{23}=\gamma_{32}=\gamma_{33}=\frac{1}{4}\frac{\Omega_2^2}{\Omega^2}\Gamma_{22}+\frac{1}{4}\frac{\Omega_1^2}{\Omega^2}\Gamma_{11}, \tag{4.12}$$
$$\gamma_{21}=\gamma_{31}=\frac{1}{2}\frac{\Omega_1^2}{\Omega^2}\Gamma_{22}+\frac{1}{2}\frac{\Omega_2^2}{\Omega^2}\Gamma_{11},$$

and the total transition rates from the states $|i,n,q\rangle$ are

$$\gamma_{1nq}=\sum_{i=1}^{3}\gamma_{1i}=0,$$
$$\gamma_{2nq}=\sum_{i=1}^{3}\gamma_{2i}=\tfrac{1}{2}\Gamma_{22}+\tfrac{1}{2}\Gamma_{11}, \tag{4.13}$$
$$\gamma_{3nq}=\sum_{i=1}^{3}\gamma_{3i}=\tfrac{1}{2}\Gamma_{22}+\tfrac{1}{2}\Gamma_{11}.$$

It is seen that the total transition rate from $|1,n,q\rangle$ is zero, indicating that there is no spontaneous emission from this state. Since there is spontaneous emission to the state $|1,n,q\rangle$ from the manifolds above, the population in the state $|1,n,q\rangle$ increases in time and for long times all population will be in this state. This effect stops the fluorescence from the Λ system and is called the coherent population trapping effect [41,42]. In order to show this more quantitatively we calculate the populations of the dressed states. For simplicity, we assume that $\Gamma_{11}=\Gamma_{22}=\Gamma$. From the quantum version of the master equation based on (2.2), we obtain a set of coupled equations for the populations P_{inq} of the dressed states. In obtaining these coupled equations the approximation [35] that dressed-atom populations are independent of q and n [apart from the factor $(\langle n_1 n_2|\alpha_1\alpha_2\rangle)^2$], together with the secular approximation, is used.

The nq is thus dropped; $P_i=\langle P_{inq}\rangle_{nq}$ is the average of P_{inq} over n,q and then the equations of motion are

$$\dot{P}_1=-\frac{\Gamma}{2}NP_1+\frac{\Gamma}{4}(N+2)(P_2+P_3),$$
$$\dot{P}_2=\frac{\Gamma}{4}NP_1-\frac{\Gamma}{4}(2N+3+|M|\cos\varphi_s)P_2$$
$$+\frac{\Gamma}{4}(N+1+|M|\cos\varphi_s)P_3, \tag{4.14}$$
$$\dot{P}_3=\frac{\Gamma}{4}NP_1+\frac{\Gamma}{4}(N+1+|M|\cos\varphi_s)P_2$$
$$-\frac{\Gamma}{4}(2N+3+|M|\cos\varphi_2)P_3.$$

The steady-state solution of Eqs. (4.14) is easily found to be

$$P_1=\frac{N+2}{3N+2},\quad P_2=P_3=\frac{N}{3N+2}. \tag{4.15}$$

It is evident from (4.15) that for the ordinary vacuum ($N=0$) the atomic population is trapped in the state $|1,n,q\rangle$. When

the atomic transition $|2\rangle$-$|1\rangle$ is coupled to a thermal or squeezed vacuum field the stimulated absorption and emission processes appear between the states $|1\rangle$ and $|2\rangle$ with the rate $N\Gamma_{11}$. These processes modify the quantum fluctuations about the frequency ω_1. Since the dressed states (4.7) contain the superpositions of the states $|2\rangle$ and $|1\rangle$ the quantum fluctuations at ω_1 are transferred into the dressed states, which leads to modifications of the transition rates between the dressed states. As a consequence, all transition rates γ_{ij} are different from zero, which results in the population of all dressed states.

According to Cohen-Tannoudji and Reynaud [35] the positions of the spectral lines and their widths are determined by the off-diagonal elements of the density operator $\rho^{(+)}_{ij,nq}$.

First we consider the sidebands at $\omega_2\pm\Omega$. Projecting the quantum version of master equation (2.2) onto $|3,n-1,q+1\rangle$ on the right and $|2,n,q\rangle$ on the left, we find that the coherences are given by

$$\dot{\rho}^{(+)}_{23}=-[i(\omega_2+\Omega)+\tfrac{1}{4}(4N+5-|M|\cos\varphi_s)\Gamma]\rho^{(+)}_{23}, \tag{4.16}$$

where the nq has been dropped, since the solutions are independent of n and q [apart from the factor related to $(\langle n_1 n_2|\alpha_1\alpha_2\rangle)^2$], and where $\rho^{(+)}_{23}=\langle\rho^{(+)}_{23,nq}\rangle_{nq}$ is the average over nq of $\rho^{(+)}_{23,nq}$.

Similarly, projecting the master equation onto $|2,n-1,q+1\rangle$ *on the right and* $\langle 3,n,q|$ on the left, and then averaging over nq, we obtain

$$\dot{\rho}^{(+)}_{32}=-[i(\omega_2-\Omega)+\tfrac{1}{4}(4N+5-|M|\cos\varphi_s)\Gamma]\rho^{(+)}_{32}. \tag{4.17}$$

The coherences (4.16) and (4.17) correspond to spectral lines at frequencies $\omega_2\pm\Omega$. The widths of these lines are

$$\lambda_{\pm\Omega}=\tfrac{1}{4}(4N+5-|M|\cos\varphi_s)\Gamma. \tag{4.18}$$

The analytical linewidths $\lambda_{\pm\Omega}$ show that the spectral lines at $\omega_2\pm\Omega$ depend on the squeezing phase φ_s, which agrees with the numerical results of Sec. III.

For the inner sidebands at $\omega_2\pm\frac{1}{2}\Omega$, we project the quantum version of the master equation (2.2) onto $|1,n-1,q+1\rangle$ on the right and $\langle 2,n,q|$ on the left, and average over nq. This results in two coupled equations:

$$\dot{\rho}^{(+)}_{21}=-[i(\omega_2+\tfrac{1}{2}\Omega)+\tfrac{1}{8}(5N+4)\Gamma]\rho^{(+)}_{21}+\tfrac{1}{4}M\Gamma\rho^{(+)}_{13}, \tag{4.19}$$
$$\dot{\rho}^{(+)}_{13}=-[i(\omega_2+\tfrac{1}{2}\Omega)+\tfrac{1}{8}(5N+4)\Gamma]\rho^{(+)}_{13}+\tfrac{1}{4}M^*\Gamma\rho^{(+)}_{21}.$$

In order to discuss linewidths and frequencies of the spectral components it is enough to find eigenvalues of Eq. (4.19). It is easy to show that the eigenvalues of Eq. (4.19) are

$$\lambda_1=\tfrac{1}{8}(5N+4+2|M|),\qquad \lambda_2=\tfrac{1}{8}(5N+4-2|M|). \tag{4.20}$$

It is seen from (4.20) that the width of the spectral line at $\omega_2+\frac{1}{2}\Omega$ depends on the squeezing parameters N and $|M|$, but is independent of the squeezing phase φ_s. This is in agreement with the numerical results of Sec. III.

The detailed coherences corresponding to the left sideband at $\omega_2-\frac{1}{2}\Omega$ can be calculated analogously. Like the right sideband at $\omega_2+\frac{1}{2}\Omega$, the left sideband has the width given in Eq. (4.20).

Finally, we consider the central component at ω_2. We project the master equation onto $|1,n-1,q+1\rangle$ on the right and $\langle 1,n,q|$ on the left and average over nq. This results in the equation of motion for the coherence $\rho^{(+)}_{11}$. It is easily verified that the coherences $\rho^{(+)}_{22}$ and $\rho^{(+)}_{33}$ oscillate with the same frequency ω_2 as $\rho^{(+)}_{11}$, and therefore have coupled equations of motion. These are readily shown to have the form

$$\begin{aligned}
\dot{\rho}^{(+)}_{11}&=-(i\omega_2+\tfrac{1}{2}N\Gamma)\rho^{(+)}_{11}+\tfrac{1}{4}(N+2)\Gamma[\rho^{(+)}_{22}+\rho^{(+)}_{33}],\\
\dot{\rho}^{(+)}_{22}&=-[i\omega_2+\tfrac{1}{4}(2N+3+|M|\cos\varphi_s)\Gamma]\rho^{(+)}_{22}+\tfrac{1}{4}N\Gamma\rho^{(+)}_{11}\\
&\quad+\tfrac{1}{4}(N+1+|M|\cos\varphi_s)\Gamma\rho^{(+)}_{33},\\
\dot{\rho}^{(+)}_{33}&=-[i\omega_2+\tfrac{1}{4}(2N+3+|M|\cos\varphi_s)\Gamma]\rho^{(+)}_{33}+\tfrac{1}{4}N\Gamma\rho^{(+)}_{11}\\
&\quad+\tfrac{1}{4}(N+1+|M|\cos\varphi_s)\Gamma\rho^{(+)}_{22},
\end{aligned} \tag{4.21}$$

and the eigenvalues of Eq. (4.21) are

$$\begin{aligned}
\eta_1&=-i\omega_2,\\
\eta_2&=-i\omega_2-\tfrac{1}{4}(3N+2)\Gamma,\\
\eta_3&=-i\omega_2-\tfrac{1}{4}(3N+4+2|M|\cos\varphi_s)\Gamma.
\end{aligned} \tag{4.22}$$

The eigenvalue η_1 corresponds to the elastic component of the spectrum, while the other eigenvalues correspond to the inelastic central components at frequency ω_2 and widths $\frac{1}{4}(3N+2)\Gamma$ and $\frac{1}{4}(3N+4+2|M|\cos\varphi_s)\Gamma$. Clearly, the linewidth of the central component depends on the squeezing phase φ_s, in agreement with the numerical calculation in Fig. 3.

The dressed-model analysis of the results presented in Figs. 4–8 for the V and cascade configurations is similar. The frequencies and intensities of the spectral features and their dependence on the squeezing phase can be explained in a similar way as the above for the Λ system.

V. SUMMARY

In this paper we have studied the phase properties of the fluorescence spectrum of a three-level atom driven by two coherent laser fields and damped by a narrow-band squeezed vacuum field. We have calculated and presented graphically the fluorescence spectra for all possible configurations of the atomic levels, i.e., the Λ, V, and cascade configurations. A phase-dependent spectrum is found when the thermal field is replaced by a squeezed vacuum field whose bandwidth is much smaller than the difference in allowed atomic transition frequencies, but much larger than atomic decay rates and Rabi frequencies of the driving fields.

In particular, we have shown that for the Λ system damped by the ordinary vacuum, coherent population trapping takes place which removes the fluorescence entirely. This is in agreement with earlier results [41–43]. When a narrow-band thermal field is applied to one of the two atomic transitions, the coherent trapping effect is destroyed and the fluorescence spectrum observed on the other transition ex-

hibits five lines, one central and two pairs of sidebands. In the case of a squeezed vacuum field, however, only the central component and the outer sidebands exhibit a dependence on the squeezing phase.

In the V configuration driven by two resonant laser fields and damped by the ordinary vacuum, the fluorescence spectrum associated with the atomic transition of frequency ω_2 exhibits three lines, a central feature at frequency ω_2 and two sidebands at $\omega_2 \pm \Omega$, where Ω is the effective Rabi frequency of the two driving fields. In the case when the other transition at ω_1 is damped by a thermal or squeezed vacuum field, additional sidebands appear in the spectrum at $\omega_2 \pm \frac{1}{2}\Omega$. Again, only the central line and the outer sidebands exhibit a dependence on the squeezing phase.

For a strongly driven cascade system and a squeezed vacuum coupled to one of the two one-photon transitions (such as the field generated by a degenerate parametric amplifier) the fluorescence spectrum reveals a phase dependence similar to that found in the Λ and V systems. However, when the squeezed vacuum is resonant to the two-photon transition between the ground and the upper excited states and coupled to both one-photon transitions also (such as the field generated by a non-degenerate parametric amplifier), all spectral lines show dependence on the squeezing phase. Thus for the cascade case a squeezed vacuum field which is the output of a nondegenerate rather than a degenerate parametric amplifier produces more extensive effects.

In order to explain the spectral features, we have applied the dressed-atom model of the system. The dressed states of the systems have been identified, and the spectral features explained in terms of transitions between these dressed states. We have shown that the unusual phase properties of the fluorescence spectra arise from the coherent mixing of the atomic states by the intense driving fields, which modifies transition rates between the dressed states.

Finally, we wish to point out that the schemes discussed in this paper, which involve three-level atoms coupled to a narrow-band squeezed vacuum whose bandwidth is much smaller than the difference in the atomic transitions frequencies, are more practical for observing the phase properties of the fluorescence spectrum, as they do not require the experimentally difficult separation of the fluorescence field from the squeezed vacuum field. Moreover, they involve a narrow-band squeezed vacuum field, which is now available in the laboratory.

ACKNOWLEDGMENTS

We would like to thank Dr. S. Swain for useful discussions. One of us (Z.F.) acknowledges the support of the Australian Research Council.

[1] N. P. Georgiades, E. S. Polzik, K. Edamatsu, H. J. Kimble, and A. S. Parkins, Phys. Rev. Lett. **75**, 3426 (1995).
[2] J. Gea-Banacloche, Phys. Rev. Lett. **62**, 1603 (1989).
[3] J. Javanainen and P. L. Gould, Phys. Rev. A **41**, 5088 (1990).
[4] Z. Ficek and P. D. Drummond, Phys. Rev. A **43**, 6258 (1991).
[5] A. S. Parkins and C. W. Gardiner, Phys. Rev. A **50**, 1792 (1994).
[6] B. R. Mollow, Phys. Rev. **175**, 1555 (1968).
[7] For a recent review, see A. S. Parkins, in *Modern Nonlinear Optics, Part II*, edited by M. Evans and S. Kielich (Wiley, New York, 1993), p. 607.
[8] C. W. Gardiner, Phys. Rev. Lett. **56**, 1917 (1986); A. S. Parkins and C. W. Gardiner, Phys. Rev. A **37**, 3867 (1988).
[9] G. J. Milburn, Phys. Rev. A **34**, 4882 (1986).
[10] G. W. Ford and R. F. O'Connell, J. Opt. Soc. Am. B **4**, 1710 (1987).
[11] G. M. Palma and P. L. Knight, Opt. Commun. **73**, 131 (1989).
[12] Z. Ficek, J. Mod. Opt. **40**, 2333 (1993).
[13] Z. Ficek and B. J. Dalton, Opt. Commun. **102**, 231 (1993).
[14] S. Smart and S. Swain, Phys. Rev. A **48**, R50 (1993); Quantum Opt. **4**, 281 (1992).
[15] G. S. Agarwal and R. R. Puri, Phys. Rev. A **41**, 3782 (1990).
[16] G. M. Palma and P. L. Knight, Phys. Rev. A **39**, 1962 (1989).
[17] J. M. Courty and S. Reynaud, Europhys. Lett. **10**, 237 (1989).
[18] Z. Ficek, W. S. Smyth, and S. Swain, Opt. Commun. **110**, 555 (1994); R. R. Tucci, *ibid*. **118**, 241 (1995).
[19] S. An, M. Sargent III, and D. F. Walls, Opt. Commun. **67**, 373 (1988).
[20] H. J. Carmichael, A. S. Lane, and D. F. Walls, J. Mod. Opt. **34**, 821 (1987).
[21] H. Ritsch and P. Zoller, Opt. Commun. **64**, 523 (1987).
[22] S. An and M. Sargent III, Phys. Rev. A **39**, 3998 (1989).
[23] A. S. Shumovsky and T. Quang, J. Phys. B **22**, 131 (1989).
[24] Z. Ficek and B. C. Sanders, Quantum Opt. **2**, 269 (1990).
[25] A. Joshi and R. R. Puri, Int. J. Mod. Phys. B **8**, 121 (1994).
[26] B. N. Jagatap, Q. V. Lawande, and S. V. Lawande, Phys. Rev. A **43**, 535 (1990).
[27] S. Smart and S. Swain, Opt. Commun. **99**, 369 (1993); J. Mod. Opt. **41**, 1055 (1994).
[28] A. S. Parkins, Phys. Rev. A **42**, 4352 (1990); **42**, 6873 (1990).
[29] J. I. Cirac and L. L. Sanchez-Soto, Phys. Rev. A **44**, 1948 (1991).
[30] H. Ritsch and P. Zoller, Phys. Rev. A **38**, 4657 (1988).
[31] See, for example, *High-Resolution Laser Spectroscopy*, edited by K. Shimoda (Springer, Berlin, 1976).
[32] P. Verkerk, B. Lounis, C. Salomon, C. Cohen-Tannoudji, J. Y. Courtis, and G. Grynberg, Phys. Rev. Lett. **68**, 3861 (1992).
[33] A. S. Parkins and C. W. Gardiner, Phys. Rev. A **40**, 3796 (1989).
[34] P. R. Rice and L. M. Pedrotti, J. Opt. Soc. Am. B **9**, 2008 (1992).
[35] C. Cohen-Tannoudji and S. Reynaud, J. Phys. B **10**, 345 (1977); C. Cohen-Tannoudji, J. Dupont-Roc, and G. Grynberg, *Atom-Photon Interactions* (Wiley, New York, 1992).
[36] M. R. Ferguson, Z. Ficek, and B. J. Dalton, J. Mod. Opt. **42**, 679 (1995).
[37] See, for example, the special issues on squeezed states: J. Mod. Opt. **34**, (6/7) (1987); J. Opt. Soc. Am. B **4** (10) (1987).
[38] M. J. Collett and C. W. Gardiner, Phys. Rev. A **30**, 1386 (1984).

[39] P. D. Drummond and M. D. Reid, Phys. Rev. A **41**, 3930 (1990).
[40] M. Lax, Phys. Rev. **172**, 350 (1968).
[41] G. Orriols, Nuovo Cimento **53**, 5 (1979).
[42] B. J. Dalton and P. L. Knight, J. Phys. B **15**, 399 (1982).
[43] D. T. Pegg, R. Loudon, and P. L. Knight, Phys. Rev. A **33**, 4085 (1986).
[44] B. R. Mollow, Phys. Rev. **188**, 1969 (1969).
[45] L. M. Narducci, G. L. Oppo, and M. O. Scully, Opt. Commun. **75**, 111 (1990); L. M. Narducci, M. O. Scully, G. L. Oppo, P. Ru, and J. R. Tredicci, Phys. Rev. A **42**, 1630 (1990); A. S. Manka, H. M. Doss, L. M. Narducci, P. Ru, and G. L. Oppo, *ibid*. **43**, 3748 (1991).
[46] Y. Zhu, Phys. Rev. A **43**, 1502 (1991).
[47] R. M. Whitley and C. R. Stroud, Jr., Phys. Rev. A **14**, 1498 (1976).